How to Cite:
Mirakhorlo, G., Nakhaei, M., Espahbod, M., Jahani, D., & Rezaei, K. (2022). Impact of formations geology factors on groundwater quality: Case study Garmsar. *International Journal of Health Sciences*, *6*(S2), 12083–12110.
https://doi.org/10.53730/ijhs.v6nS2.8146

Impact of formations geology factors on groundwater quality: Case study Garmsar

Gohar Mirakhorlo
Ph.D. Student, Department of Geology, North Tehran Branch, Islamic Azad University, Tehran, Iran
Email: goharmira@gmail.com

Mohammad Nakhaei
Professor, Department of Geology, Kharazmi University, Hesarak Karaj, Corresponding Author, Karaj, Iran
Corresponding author email: nakhaeimohammad@gmail.com

Mohammadreza Espahbod
Associate Professor, Department of Geology, North Tehran Branch, Islamic Azad University, Tehran, Iran
Email: mr_esphbod@iau-tnb.ac.ir

Davoud Jahani
Associate Professor, Department of Geology, North Tehran Branch, Islamic Azad University, Tehran, Iran
Email: d_jahani@iau-tnb.ac.ir

Khalil Rezaei
Associate Professor, Department of Geology, Kharazmi University, Hesarak Karaj, Karaj, Iran
Email: kh.rezaei@gmail.com

***Abstract*---**Garmsar plain is one of the central desert sub-basins in Semnan province with a warm and dry desert climate. After the HablehRood River, which is the main source of surface water of the area, the groundwater resources of Garmsar plain have a vital role in supplying agricultural and industrial demands; hence, the quality assessment of the groundwater is very important since it has a very great impact on the environment. This study aims to analyze the water quality of the area and determine the effects of geological formations on the hydrochemical deterioration of the groundwater quality in the area. To this aim, the hydrochemical environment of the region was simulated using Qa.Aq, Rockwors16, and GIS10.1 using the upstream of the basin chemical water and groundwater

Manuscript submitted: 09 March 2022, Manuscript revised: 18 April 2022, Accepted for publication: 27 May 2022

hydrochemistry data, the Garmsar study area was simulated. Besides, mineral saturation indices, hydrochemical water facies, and the total amount of soluble materials were determined, and the diagram of one or more effective hydrochemical variables was drawn. The results show that the most important factor in groundwater quality is the interaction between water and geological facies. Salt and gypsious formations (especially lower red formation) in the northern part of the plain lead to gradual changes of the water type to Chloride. Fine-grain formation (upper red member) leads to ion exchange and an increase of solvable ions in the water.

***Keywords*---**geological formations, groundwater quality, aquifer, saturation index.

Introduction

Groundwater quality is affected by natural processes and human activities. Groundwater is always contaminated by human activities such as agriculture and urban and industrial wastewater, and since groundwater contamination is dynamic, costly, and difficult to improve, it is vital to protect it. (Fatima, A., et. al., 2021; Hassanin SO, et. al., 2019) The rapid population growth, the spread of polluting industries, the uneven development of cities, and human activities have created a critical state in water resources. Hydrogeochemistry studies the reactions that occur between the water phase and stone phase under the ground. By understanding the geochemical processes governing the aquifer of an area, one can provide insight into the changes in the concentration of constituents soluble in groundwater along the flow path and better describe their temporal and spatial variations. According to Anderson et al. (1988) and Appelo and Postma (2005), the chemical properties of groundwater in a basin are affected by deposited sediments, evaporation and perspiration, area topography, nutrient composition, and drought and wet status. There have been many studies on groundwater quality and its controlling factors, including studies by Van der Weijden et al. (2003), Jalali (2007), Jalali (2005), Sasamoto et al. (2004).

Busby et al. (1991) also used saturation index relationships to investigate the aquifer hydrochemistry in Madison, South Dakota. Sandow Mark (2009) has analyzed the groundwater quality by multivariate and statistical methods. Faryabi et al. (2010) have investigated the hydrochemistry of Ovan plain using saturation index and factor analysis method. Flak et al. (2011) examined the impacts of geology and human on the groundwater flow system in the slope and basin in the Selva Basin (Catalonia, NE Spain). The assessment of groundwater quality changes in most countries of the world is a relatively new issue (Rosen and Lapham, 2008). In order to identify such processes, it is necessary to study the concentration of groundwater bodies in each study area. Garmsar lies between 35° 5′, 35° 17′ N latitude, 52° 15′, and 52° 35′ E longitude from the Greenwich meridian in Semnan province (Figures 1, 2).

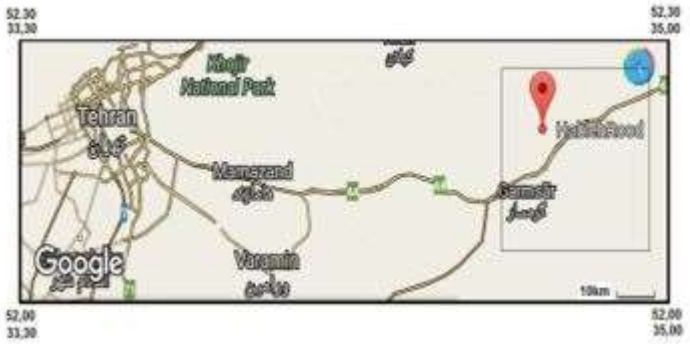

Figure 1. Geographical location of Garmsar

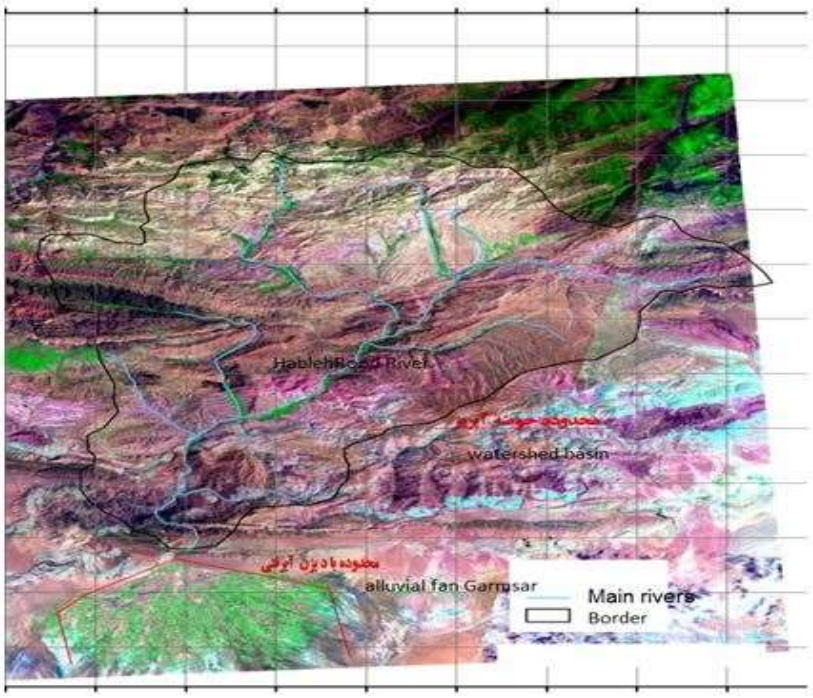

Figure 2. Location of the watershed basin and Garmsar alluvial fan area.

The Garmsar study area climate ranges from cold mountainous to warm and arid desert climate. The northern elevations of the basin include central Alborz, which enjoys cold to temperate mountain climates. Garmsar plain is almost located in the lowest and southern parts of the basin and is dominated by a warm and dry desert climate. The mean annual rainfall in the highlands and plain is 200.9 mm and 81.4 mm, respectively. The amount of evaporation from the pan in the plain and the elevations of the study area were calculated to be 2903 mm and 2030.1 mm, respectively. According to the Semnan Regional Water Company statistics, and based on the census of 2009, 897 wells with an annual discharge of 139.1 million cubic meters, 47 aqueducts with a discharge of 1.97 million cubic meters,

and 361 spring openings with an annual discharge of 17.92 million cubic meters have been identified. The share of elevations in these statistics includes 365 wells with an annual discharge of 10.76 million cubic meters, 18 aqueducts with a discharge of 0.54 million cubic meters per year, and 361 wells with an annual discharge of 17.92 million cubic meters. Five hundred twenty-three wells with an annual discharge of 127.75 million cubic meters and 28 aqueducts with a discharge of 1.1 million cubic meters per year have been identified in Garmsar alluvial aquifer. The total volume of discharge and harvesting of groundwater resources identified in the Garmsar alluvial aquifer is 128.86 million cubic meters per year.

Geology and Tectonics

According to the geological six divisions of Stocklin (1968), the Garmsar plain is classified in the Central Iran Zone. The HableRood River watershed is geographically located on the southern slope of the central Alborz Mountains. Nevertheless, in terms of construction and extension of the formations (especially in the southern part) as well as the longtime geography, it has some characteristics that some geologists, including Berberian and King (1981), place in the Alborz area (Aghanabati, 2011, p. 583).

Stratigraphy

In terms of stratigraphy and lithology, the HableRood River basin is one of the oldest formations to the present age (Figure 3). The Kahar Formation is at the end of the western and eastern parts of the basin, and its lithology is gray clay silty shales with the Precambrian age.

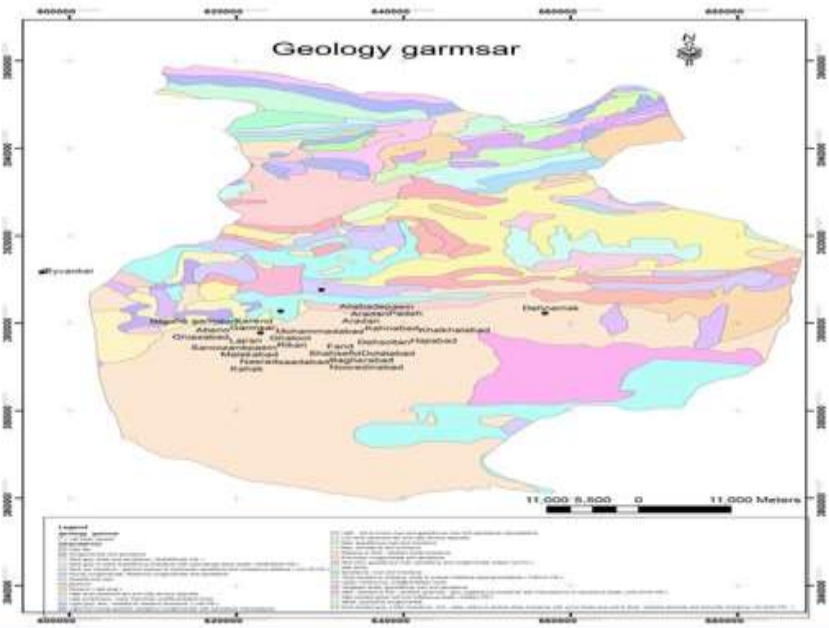

Figure 3. Geology of Garmsar Study Area (Goharmirakrlo-2018) Adapted from the Geological Survey of Iran

Some formations of the first era are the Mubarak organizations and the formations of Dorud and Rute. The lithology of the Mubarak Formation is black lime, while Dorud Formation is composed of conglomerate, shale, lime, sandstone. The lithology of the Ruteh Formation is also composed of dark gray lime and marl thin layers. Elika formation with Triassic age is composed of thin-layer limestone and thick calcareous dolomitic layers. Melaphyres that are output thin stones are located on the Elika Formation and outcrop in the western part of the HablehRood Basin. The age of these Melaphyres is of the Upper Triassic. The Shemshak Formation consists of shale, sandstone, and marl with thick coal layers in the western- northwestern, along the Firouzkouh Abik fault, and the middle parts of the basin. The Delichai Formation is present in the eastern-northeastern, western, and middle parts of the basin with marl lime and green marl lithology. The Lar Formation, with and extension similar to the Delichai Formation, can be seen in the basin. The age of the above formation is Upper Jurassic and is composed of thick-layer dolomite and gray dolomitic-limestone layers lithology.

Due to the orogenic phase function, equivalent to the Late Cimmerian, the Lower Cretaceous formations have not been formed in the area, and the Upper Cretaceous formations are located on the Lar Formation with isocline discontinuity. The lithology of these rocks is often lime and shale lime. Paleogene formations have a relatively large extent in the region and cover the basin from north to south; from old to new, they are:
Fajan Formation: It is composed of polygenetic conglomerates with abundant crustaceans, shale, sandstone, marl, and calcareous yellow layers above.
Ziarat Formation: It consists of thin to thick lime layers.
Karaj Formation: It has the greatest extent; most of the distributaries that provide water to the HablehRood River erode part of this formation carrying it downstream. Its lithology consists of a sequence of shale-green tuff sandstone and thick tuff sandstone with layers of green to gray-yellow shales. Plaster horizons can be seen at the top.
Neogene formations include:
Qom Formation: It is so extensive, including a sequence of lime, green marl, and evaporite sediments.
Upper Red Formation: It is the thickest and widest formation in the basin, with a thickness of more than 6,000 meters in the area and generally consisting of shale, marl, sandstone, and plaster in red-gray and green colors. On these sediments, there are layers of light brown and gray mudstone and sandstone with gypsum cement and conglomerate-shaped lens layers.
In the watershed and adjacent basins, there are numerous salt domes originating from the Lower Red Formation. The passage of the HablehRood River through these domes, as well as the drainage of water of these domes into the HablehRood River, has made the water quality of the river largely poor.
Hezar Dare Formation: It includes calcareous crusts of Qom Formation, upper red formation sandstones, and volcanic rocks, as well as older rubbles that are linked by sandstone matrix, salt clay-gypsum cement. This formation in the watershed is highly extended from east to west. The recently mentioned formations have the largest contributions to the sediment supply in the Garmsar plain.
Young alluviums: They contain very young alluvial deposits and are composed of rubbles, pebbles, and sand. These sediments lie in the bed of seasonal waterways

and main rivers. The above alluviums are disintegrated and have great porosity and permeability (Semnan Regional Water Company, 2016).

Materials and Methods

The first step is to visit the Semnan Regional Water Company, collect available statistics, information, and reports, plan more accurately to complete the sampling quality network and evaluate the nitrate ion concentration as an indicator of the contamination of the studied area. The next step is a sampling from the study area; in this step, it was attempted to collect data for the region and aquifer indicator and to deliver them to the laboratory within 48 hours. The electrical conductivity, pH, and temperature of the samples were measured in the desert. In the next step, we tried to study and process the data collected from the area in the office using the most commonly used software in the world (excel, chimistre, ArcGis, Rockworks, Aqqa, PhreeQc software). Finally, the plain hydrochemistry report was prepared, and the results of these studies will be presented below. As all waters reach the sea at the end, according to Chebotarev (1995), waters tend to evolve chemically toward seawater. He observed that this evolution is usually accompanied by regional changes in the dominant anionic compounds as follows:

Moving along the flow path

$HCO_3 \rightarrow HCO_3 + SO_4 \rightarrow SO_4 + HCO_3 \rightarrow SO_4 + Cl \rightarrow Cl + SO_4 \rightarrow Cl$

Increasing shelf life

These changes occur in terms of water movement from saturated areas with active currents to intermediate regions and eventually to areas where the flow is very slow, and water is old. The results of the analysis of water samples taken during two stages of the dry and wet season in October and March were used (Figure 4). Samples included 33 groundwater sources (wells), 30 in Garmsar plain and 3 in Firouzkooh, and 9 surface water sources. The results of chemical measurements of groundwater samples are presented in Table 1.

Table 1. Validation results of water samples in March 2018.

R	NAME	Time	UTMX	UTMY	EC	T.D.S	PH	Meq Ca	Meq Mg	Meq Na	Meq K	total-cation	Meq HCO3	Meq CO3	Meq CL	Meq SO4	No3-	Total anion	error%	
w1	balochy	2018/03/07	612994	3894598	7630	4960	7.7	14.80	8.40	60.90	0.50	84.60	2.10	0.00	70.63	7.34	0.37	80.07	2.75	2018/03/07
w2	razvan	2018/03/07	614736	3892372	6230	4050	8	20.20	14.60	52.20	0.35	87.35	3.50	0.00	57.38	20.19	0.74	81.07	3.73	2018/03/07
w3	zali	2018/03/07	616440	3897028	9840	6396	6.94	40.50	21.50	72.50	0.59	135.09	3.35	0.00	94.38	24.67	0.56	122.40	4.93	2018/03/07
w4	shaeri	2018/03/07	617455	3892816	7710	5012	7.29	24.00	20.40	58.00	0.48	102.88	4.95	0.00	68.38	21.37	0.66	94.70	4.14	2018/03/07
w5	ertefahi	2018/03/07	618204	3895201	3700	2405	7.45	11.70	6.20	35.37	0.23	53.50	1.95	0.00	46.75	7.69	0.40	56.39	-2.63	2018/03/07
w6	sarsabz	2018/03/09	620682	3889625	4960	3224	7.05	11.65	10.10	30.28	0.28	52.31	4.15	0.00	34.15	12.59	0.33	50.89	1.38	2018/03/09
w7	chastniko	2018/03/09	620620	3886869	7920	5148	6.85	17.30	17.30	52.58	0.62	87.80	5.40	0.00	54.38	35.50	0.32	95.28	-4.09	2018/03/09
w8	saberdari	2018/03/03	622436	3899220	3160	2054	7.96	7.95	6.20	21.03	0.20	35.38	5.65	0.00	20.63	9.47	1.04	35.75	-0.52	2018/03/03
w9	kusk-a	2018/03/03	622895	3896458	3290	2139	7.76	4.40	3.30	30.23	0.19	38.12	3.20	0.00	27.48	6.69	0.53	37.37	0.99	2018/03/03
w10	mnahehtabili	2018/03/08	624531	3901427	2460	1599	7.8	4.80	3.90	26.10	0.16	34.96	3.85	0.00	16.43	11.27	0.36	31.55	5.12	2018/03/08
w11	Kallah vardiahad	2018/03/07	624842	3895723	4720	3068	7.32	5.85	5.00	42.17	0.23	53.25	4.00	0.00	37.75	12.96	0.31	54.71	-1.35	2018/03/07
w12	mandolak-a	2018/03/07	626021	3892629	3450	2243	7.66	7.35	5.00	26.24	0.56	39.15	3.00	0.00	27.55	8.37	0.64	38.92	0.29	2018/03/07
w13	burun	2018/03/07	625584	3890290	6250	4063	7.14	15.80	13.80	43.50	0.25	73.35	7.85	0.00	51.63	8.43	0.51	67.91	3.85	2018/03/07
w14	alivaliollah	2018/03/07	626905	3889472	4080	2652	7.32	8.50	8.70	28.53	0.27	46.00	4.35	0.00	29.45	10.26	0.67	44.06	2.15	2018/03/07
w15	hagiabad-a	2018/03/07	627686	3901023	5260	3419	7.4	13.40	6.60	17.40	0.20	37.60	2.00	0.00	32.00	7.12	0.35	41.12	-4.47	2018/03/07
w16	k-hasanabad	2018/03/07	629126	3896126	2200	1430	7.44	6.20	3.60	17.40	0.16	27.36	2.80	0.00	16.88	6.38	0.41	26.06	2.44	2018/03/07
w17	fatholmobin	2018/03/02	630297	3887889	3380	2197	7.04	9.90	9.00	29.00	0.23	48.13	3.15	0.00	30.75	10.84	0.34	44.74	3.65	2018/03/02
w18	k-ghashlagh haghi	2018/03/02	631113	3897091	2450	1593	7.45	8.70	5.50	13.05	0.17	27.42	2.70	0.00	19.53	7.84	0.63	30.07	-4.62	2018/03/02
w19	k-hastabad	2018/03/02	633140	3901150	1840	1196	7.38	8.00	3.80	11.60	0.15	23.55	1.90	0.00	12.48	7.29	0.27	21.67	4.16	2018/03/02
w20	dolatabad	2018/03/02	636509	3895110	2310	1502	7.26	7.70	4.80	14.43	0.16	27.09	3.20	0.00	14.63	7.85	0.31	25.68	2.67	2018/03/02
w21	khadamat	2018/03/02	636132	3898452	1415	920	7.73	5.80	6.20	11.10	0.14	23.24	1.50	0.00	13.23	7.72	0.22	22.45	1.72	2018/03/02
w22	dastani	2018/03/02	638210	3891277	2350	1528	7.58	7.00	4.30	13.29	0.16	24.75	2.20	0.00	15.03	8.71	0.27	25.94	-2.34	2018/03/02
w23	dehpiran	2018/03/02	639077	3893050	2124	1381	6.96	12.20	10.40	22.13	0.23	44.96	5.20	0.00	25.25	14.00	0.39	44.45	0.57	2018/03/02
w24	padeh-a	2018/03/02	638313	3901916	1963	1276	7.51	7.30	4.30	13.05	0.12	24.77	2.20	0.00	15.03	8.43	0.20	25.66	-1.76	2018/03/02
w25	amamzadeh zolfaghar	2018/03/02	640529	3896361	2600	1690	7.15	9.60	6.95	16.85	0.25	33.65	4.30	0.00	18.28	9.11	0.37	31.69	2.99	2018/03/02
w26	farvan	2018/03/02	640196	3899568	1670	1086	7.02	5.60	3.30	13.05	0.19	22.14	2.35	0.00	10.93	6.72	0.42	20.00	5.08	2018/03/02
w27	samsi	2018/03/02	641157	3894165	5810	3777	6.75	17.9	19.95	37.24	0.42	75.51	6.1	0	38.95	31.86	0.28	76.91	-0.92	2018/03/02
w28	daneh	2018/03/02	642848	3902078	4850	3153	6.98	14	10.1	21.41	0.23	45.74	3	0	29.15	15.84	0.25	47.99	-2.41	2018/03/02
w29	gholam sah	2018/03/02	643089	3898298	2680	1742	6.94	4	5.85	19.62	0.20	29.67	2.5	0	15.78	12.53	0.31	30.81	-1.88	2018/03/02
w30	bostan	2018/03/02	643350	3892288	3030	1970	7.64	5.9	7.3	20.62	0.27	34.09	2.8	0	19.33	11.23	0.19	33.36	1.09	2018/03/02
w31	hablehrood	2018/03/02	628672	3907245	650	423	8.9	4.2	3.8	10.2	0.15	18.35	2.5	1	9	6.3	0.19	18.80	-1.22	2018/03/02
w32	saridareh	2018/03/02	628687	3907598	13000	8450	8.5	120	90	1230	18.34	1458.34	2.8	6	1320	59	0.88	1387.80	2.48	2018/03/02
w33	gholamah	2018/03/02	629224	3917880	20000	13000	6	29	22	167	1.10	219.10	3	1	205	3.4	0.22	212.40	1.55	2018/03/02
w34	rashidsoltan	2018/03/02	629670	3920903	659	428	8.92	2.56	2.2	5	0.04	9.80	3.13	0	3.7	3.1	0.26	9.93	-0.66	2018/03/02
w35	simindast	2018/03/02	635739	3931578	630	410	9.27	3.3	2.8	0.3	0.04	6.44	4.4	0	0/8	1.03	0.29	6.23	1.66	2018/03/02
w36	zodafshoon	2018/03/02	632969	3942018	630	410	9.22	1.39	0.67	0.79	0.04	2.89	1.88	0	0.28	0.53	0.33	2.69	3.66	2018/03/02
w37	dalichay	2018/03/02	635431	3948871	364	237	8.38	2.6	1.28	2.14	0.04	6.06	3	0	2	0.9	0.26	5.90	1.30	2018/03/02
w38	namrood	2018/03/02	650477	3953481	317	206	8.57	2.04	0.45	0.76	0.05	3.30	1.56	0.43	0.38	0.86	0.22	3.23	1.02	2018/03/02
w39	aminabad	2018/03/02	642763	3949063	103	67	8.5	2.01	0.4	0.9	0.03	3.34	1.55	0.4	0.37	0.84	0.37	3.16	2.70	2018/03/02
w40	Kosta rghah	2018/03/02	651927	3955793	627	408	8.75	3.55	1.73	1.69	0.08	7.05	4.12	0.4	0.92	1.5	0.44	6.94	0.78	2018/03/02
w41	vahdat	2018/03/02	628326	3946687	411	267	8.76	3.14	0.72	1.36	0.03	5.25	3/2	0.4	0.58	0.86	0.35	44258.84	-99.98	2018/03/02
w42	ghoorsafid	2018/03/02	670307	3959175	468	304	8.26	2.7	1.6	0.6	0.05	4.95	3.9	0.5	0.3	0.3	0.23	5.00	-0.49	2018/03/02
w43	Firooz kooh	2018/03/02	656008	3948650	540	351	8.8	2.93	2.85	0/9	0.08	6.76	4.4	0.5	0.4	1.03	0.29	6.33	3.27	2018/03/02
w44	sprin	2018/03/02	652315	3947346	1371	891	7.6	4.1	3.25	4.2	0.21	11.76	3.75	0.2	3.4	3.9	0.23	11.25	2.22	2018/03/02

Figure 4. Location of the sampled water

According to Hounslow (1995) and Schwartz and Zhang (2003), the acceptable rate of reaction error is 5%, but other researchers such as Mazor (1992) have suggested it to be 10%. The maximum reaction error of the study area was 5.17% for the w26 sample in October.

Discussion and Conclusion

Hydrogeochemical facies are distinct fractions with cationic and anionic concentrations that can be described in certain compositional groups (Freeze and Cherry, 1979). The basis of the facies classification is the number of major cations and anions (in meq/l) of groundwater (Sikdar et al., 2001). Groundwater and surface water types in Garmsar are chlorinated, while they are two types of bicarbonate and sulfate in Firoozkooh wells. Based on the Piper diagram (Figure 5), there are four sources for groundwater that are identified by four hydrochemical facies. (Na-cl, Na-Hco_3, ca-so_4, and Ca-Hco_3).

1. $Ca^{2+} - SO_4^{2-}$: Gypsum stones specific waters containing gypsum and anhydrite and mine drainage.
2. $Ca^{2+} - HCO_3^-$: Shallow and sweet waters
3. $Na^+ - Cl^-$: Waters of marine origin as well as fossil waters.
4. $Na^+ - HCO_3^-$: Deeper waters affected by ion exchange.

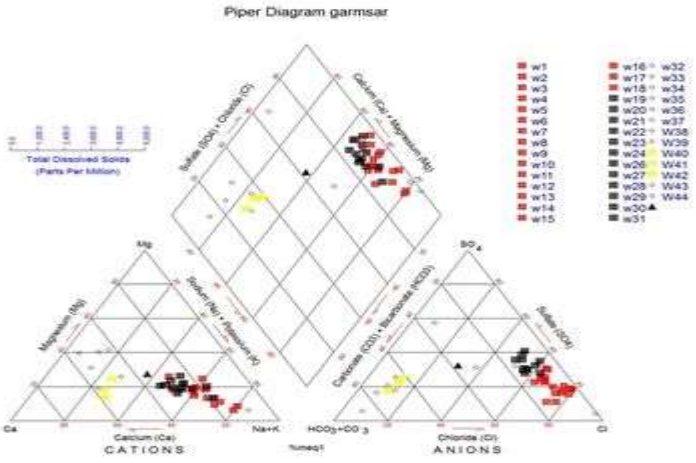

Figure 5. Piper diagram of water samples.

According to the Durov diagram of the study area, there is an evolutionary trend (Figure 6) so that in the northern parts (Firouzkouh), the surface water type is bicarbonate, while it is chlorinated when going towards the output of the studied area. A stiff diagram of the area's water sample was drawn using Rockworks software (Figure 7).

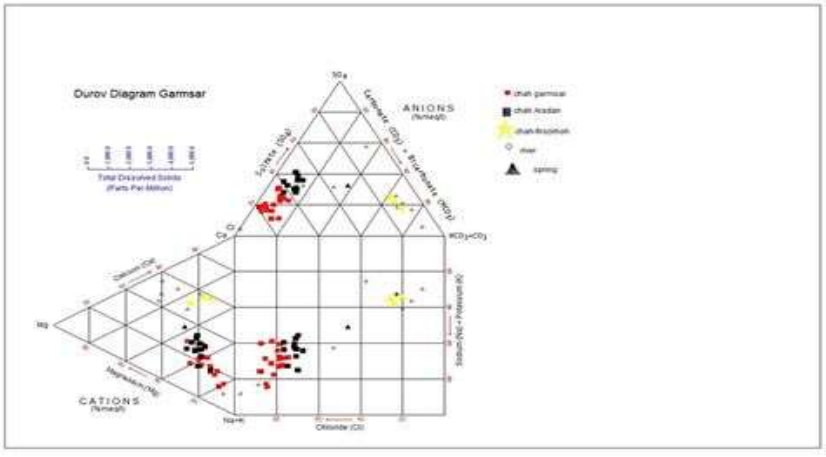

Figure 6. Durov diagram of Study Area in March 2018.

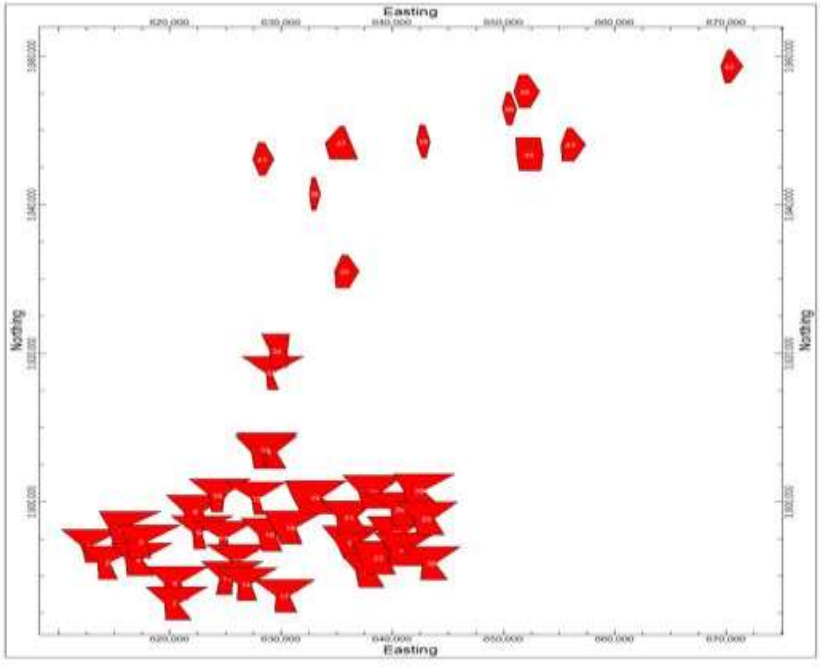

Figure 7. Stiff diagram of Garmsar study area.

Using ion ratios in determining the origin of salinity

Ion ratio of $\frac{Na^+}{Na^+ + Cl^-}$ is used to determine the origin of the salinity of groundwater. The ratio value ranges from 0.35 to 0.72, with a mean value of 0.51 (Table 2). The value of this ionic ratio indicates that the salinity of groundwater in this area can be due to the dissolution of halite (Hounslow, 1995). Values greater than 0.5 in some samples of water can indicate the process of sodium and

calcium ion exchange. Ion ratio of $\frac{Ca^{2+}}{Ca^{2+}+SO_4^{2-}}$ ranges from 0.24 to 0.90 with a mean value of 0.53 (Table 2) and indicates the gypsum dissolution in the aquifer. In addition, the Ion ratio of $\frac{Ca^{2+}+Mg^{2+}}{SO_4^{2-}}$ in the groundwater passing through evaporite rocks (gypsum and anhydrite) is close to the unit value (Richter and Kreitler, 1993). The values of this ionic ratio in the waters range from 0.77 to 14.33, with a mean of 2.41.

Table 2. Ionic ratio of water samples in March 2018

X	Y	Abbreviation	Na/(Na+Cl)	Ca/(ca+so4)	(Ca+mg)/Hco3	(ca+mg)/so4	hco3/cl	hco3/so4	mg/ca	so4/cl	ca+mg	hco3+so4	Na/cl	Ca/Mg	cl/hco3+co3	No3mg/l	so4/hco3
612994	3894598	w1	0.46	0.67	11.05	3.16	0.03	0.29	0.57	0.10	23.20	9.44	0.86	1.76	33.63	23.5	3.50
614736	3892372	w2	0.48	0.50	9.94	1.72	0.06	0.17	0.72	0.35	34.80	23.69	0.91	1.38	16.39	46.9	5.77
616440	3897028	w3	0.43	0.62	18.51	2.51	0.04	0.14	0.53	0.26	62.00	28.02	0.77	1.88	28.17	35.2	7.36
617455	3892816	w4	0.46	0.53	8.97	2.08	0.07	0.23	0.85	0.31	44.40	26.32	0.85	1.18	13.81	41.6	4.32
618204	3895201	w5	0.43	0.60	9.18	2.33	0.04	0.25	0.53	0.16	17.90	9.64	0.76	1.89	23.97	25.4	3.94
620682	3889625	w6	0.47	0.48	5.24	1.73	0.12	0.33	0.87	0.37	21.75	16.74	0.89	1.15	8.23	20.7	3.03
620620	3886869	w7	0.49	0.33	6.41	0.97	0.10	0.15	1.00	0.65	34.60	40.90	0.97	1.00	10.07	20.3	6.57

62436	389922 0	w8	0.50	0.46	2.50	1.49	0.27	0.60	0.78	0.46	14.15	15.12	1.02	1.28	3.65	65.6	1.68
62895	389645 8	w9	0.52	0.40	2.41	1.15	0.12	0.48	0.75	0.24	7.70	9.89	1.10	1.33	8.59	33.2	2.09
62531	390142 7	w10	0.61	0.30	2.26	0.77	0.23	0.34	0.81	0.69	8.70	15.12	1.59	1.23	4.27	22.7	2.93
62842	389572 3	w11	0.53	0.31	2.71	0.84	0.11	0.31	0.85	0.34	10.85	16.96	1.12	1.17	9.44	19.5	3.24
62021	389262 9	w12	0.49	0.47	4.12	1.48	0.11	0.36	0.68	0.30	12.35	11.37	0.95	1.47	9.18	40.1	2.79
62584	389029 0	w13	0.46	0.65	3.77	3.51	0.15	0.93	0.87	0.16	29.60	16.28	0.84	1.14	6.58	32.1	1.07
62905	388947 2	w14	0.49	0.45	3.95	1.68	0.15	0.42	1.02	0.35	17.20	14.61	0.97	0.98	6.77	41.9	2.36
62686	390102 3	w15	0.35	0.65	10.00	2.81	0.06	0.28	0.49	0.22	20.00	9.12	0.54	2.03	16.00	22.3	3.56
62926	389612 6	w16	0.51	0.49	3.50	1.54	0.17	0.44	0.58	0.38	9.80	9.18	1.03	1.72	6.03	25.9	2.28
63097	388788 9	w17	0.49	0.48	6.00	1.74	0.10	0.29	0.91	0.35	18.90	13.99	0.94	1.10	9.76	21.4	3.44
63113	389709 1	w18	0.40	0.53	5.26	1.81	0.14	0.34	0.63	0.40	14.20	10.54	0.67	1.58	7.23	39.8	2.90
63140	390115 0	w19	0.48	0.52	6.21	1.62	0.15	0.26	0.48	0.58	11.80	9.19	0.93	2.11	6.57	17	3.84
63	38	w	0	0.	3.9	1.5	0.	0.	0	0	12	1	0.	1	4.	1	2.

6509	9511 0	20	.50	50	1	9	22	41	.62	.54	.50	1.05	99	.60	57	9.3	45
6361 32	3898 452	w21	0.46	0.43	8.00	1.55	0.11	0.19	1.07	0.58	12.00	9.22	0.84	0.94	8.82	14	5.15
6382 10	3891 277	w22	0.47	0.45	5.14	1.30	0.15	0.25	0.61	0.58	11.30	10.91	0.88	1.63	6.83	17.3	3.96
6390 77	3893 050	w23	0.47	0.47	4.35	1.61	0.21	0.37	0.85	0.55	22.60	19.20	0.88	1.17	4.86	24.6	2.69
6383 13	3901 916	w24	0.46	0.46	5.27	1.38	0.15	0.26	0.59	0.56	11.60	10.63	0.87	1.70	6.83	12.5	3.83
6405 29	3896 361	w25	0.48	0.51	3.85	1.82	0.24	0.47	0.72	0.50	16.55	13.41	0.92	1.38	4.25	23.4	2.12
6401 96	3899 568	w26	0.54	0.45	3.79	1.32	0.22	0.35	0.59	0.61	8.90	9.07	1.19	1.70	4.65	26.2	2.86
6411 57	3894 165	w27	0.49	0.36	6.20	1.19	0.16	0.19	1.11	0.82	37.85	37.96	0.35	0.90	6.39	17.5	5.22
6428 48	3902 078	w28	0.42	0.47	8.03	1.52	0.10	0.19	0.72	0.54	24.10	18.84	0.73	1.39	9.72	15.8	5.28
6430 89	3898 298	w29	0.55	0.24	3.94	0.79	0.16	0.20	1.46	0.79	9.85	15.03	1.24	0.68	6.31	19.4	5.01
6433 50	3892 288	w30	0.52	0.34	4.71	1.18	0.14	0.25	1.24	0.58	13.20	14.03	1.07	0.81	6.90	12	4.01
6286 72	3907 245	w31	0.53	0.40	3.20	1.27	0.28	0.40	0.90	0.70	8.00	8.80	1.13	1.11	2.57	12.2	2.52
6286	3907	w32	0.	0.54	49.64	2.36	0.0	0.0	1.	0.	139.	61.	0.9	0.	352.	55	21.

87	598		48				0	5	01	02	00	80	1	99	56	.7	07
629224	3917880	w33	0.46	0.47	1.67	1.47	0.15	0.88	0.67	0.17	5.00	6.40	0.84	1.50	5.05	13.6	1.13
629670	3920903	w34	0.72	0.51	1.04	1.62	3.14	1.56	0.56	2.01	7.12	11.23	2.51	1.78	0.32	16.6	0.64
635739	3931578	w35	0.43	0.74	1.30	5.53	11.00	4.27	0.97	2.58	5.70	5.43	0.75	1.04	0.09	18.4	0.23
632969	3942018	w36	0.72	0.72	1.10	3.89	6.71	3.55	0.48	1.89	2.06	2.41	2.61	2.07	0.15	20.8	0.28
635431	3948871	w37	0.52	0.73	1.29	4.04	1.50	3.13	0.49	0.48	3.88	3.96	1.07	2.03	0.67	16.4	0.32
650477	3953481	w38	0.67	0.70	1.60	2.90	4.11	1.81	0.22	2.26	2.49	2.42	2.00	4.53	0.19	14	0.55
642763	3949063	w39	0.65	0.71	1.55	2.87	4.19	1.85	0.20	2.27	2.41	2.39	1.89	5.03	0.19	23.3	0.54
651927	3955793	w40	0.63	0.70	1.19	3.28	5.72	2.75	0.41	2.08	4.92	5.62	1.68	2.46	0.16	27.8	0.36
628326	3946687	w41	0.70	0.79	1.13	4.60	6.03	4.07	0.22	1.48	3.96	4.36	2.34	4.50	0.15	22.2	0.25
670307	3959175	w42	0.67	0.90	1.10	14.33	13.000	13.000	0.59	1.00	4.30	4.20	2.00	1.69	0.07	14.2	0.08
656008	3948650	w43	0.43	0.74	1.27	5.44	11.00	4.27	0.93	2.58	5.60	5.43	0.75	1.07	0.08	18.3	0.23
652315	394734	w44	0.5	0.59	1.35	2.24	1.21	1.66	0.5	0.7	7.18	8.50	1.12	1.7	0.83	14.	0.60

	6		3						9	3				0		5	

The origin of calcium and magnesium ions in groundwaters can be determined by the ion ratio $(Ca^{2+}+Mg^{2+})/HCO_3^-$. As this ion ratio corresponds to the increase in TDS values, calcium and magnesium ions are added to the solution in greater proportion than bicarbonate ions. If the calcium and magnesium ions are only derived from dissolution of carbonates and minor minerals (pyroxene and amphibole), this ratio is approximately 0.5, which is created due to the carbon dioxide reaction from atmospheric origin or corrosion of soil organic matter with carbonate rocks.
The oxidation of organic matter and respiration of plants' roots produce CO_2 in the unsaturated zone and dissolve it in groundwater in the feeding zone. Some amounts of CO_2 can be in bicarbonate ions (Wen et al., 2005). Drawing values of ($Ca^{2+}+Mg^{2+}$) vs. HCO_3^- of groundwaters shows that most data are above the 1:1 line.

Despite the fact that a high ion ratio of $(Ca^{2+}+Mg^{2+})/HCO_3^-$ cannot be attributed to the reduction of bicarbonate ions, under alkaline conditions, HCO_3^- ion of groundwater cannot be created from H_2CO_3 reaction (Spears, 1986). The ion ratio values range from 1.04 to 49.64, with a mean of 5.63. The high values of this ionic ratio in the waters of the area may indicate that the excess amounts of alkalinity of such waters are balanced by $Na^+ + K^+$ cations. Excess amounts of ($Ca^{2+}+Mg^{2+}$) vs. HCO_3^- indicates the supply of calcium and magnesium ions from another source, such as reverse ion exchange or dissolution of sulfates. $Ca^{2+}+Mg^{2+}$ ions in the groundwater of the area could be balanced by the $Cl^- + SO_4^{2-}$ ions. The extension of the evaporite deposits of the lower and upper Red Formation can provide sodium and chlorine ions in the region's waters. (Figures 8 and 9).

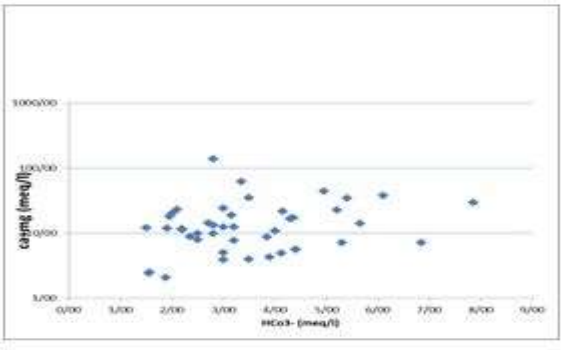

Figure 8. Drawing values of $Ca^{2+}+Mg^{2+}$ vs. bicarbonate ions.

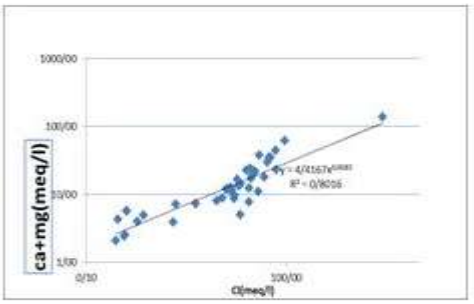

Figure 9. Drawing values of $Ca^{2+} + Mg^{2+}$ vas. Chlorine ions

Salinity is the total amount of inorganic solids soluble in natural water, indicating an increase in TDS and an increase in the concentration of chemical components soluble in water (Richter and Kreitler, 1993). Ion ratios of $\frac{Na^+}{Cl^-}$, $\frac{SO_4^{2-}}{Cl^-}$, $\frac{Ca^{2+}}{HCO_3^- + SO_4^{2-}}$, and $\frac{Mg^{2+}}{Ca^{2+}}$ are used to identify different sources of salinity of groundwater. Groundwater salinity in the aquifer can be influenced by the following factors (Ghabayen et al., 2006).

1) The influx of sea salt water into the aquifer
2) Upconing of saline waters from deeper parts of the aquifer
3) Water flows through the marl and gypsum sediments
4) Return water from municipal wastewater
5) Oil brines and the impact of salt domes

The geochemical changes of such salinity waters can occur because of water-rock reactions. These reactions can include the following cases (Vengosh et al., 1999; Ghabayen et al., 2006):

a) Basic ion exchange reactions with clay minerals that reduce the amount of sodium and increase the amount of calcium and magnesium in the water. Because of this process, the $\frac{Na^+}{Cl^-}$ ion ratio decreases while the $\frac{Ca^{2+}}{HCO_3^- + SO_4^{2-}}$ ion ratio increases.

b) Adsorption by clay minerals that can affect the potassium concentration of the water.

c) Dissolution - deposition of carbonate minerals, which increases the concentration of calcium ion and decreases the concentration of bicarbonate. Increased calcium concentration due to the process of basic ion exchange and dissolution of carbonate minerals increases $\frac{Ca^{2+}}{HCO_3^- + SO_4^{2-}}$ ionic ratio to more than one unit, which may indicate the presence of calcium-chloride deposits. $\frac{SO_4^{2-}}{Cl^-}$ ion ratio is not unaffected by this process and mainly acts as a conservative indicator. Groundwater enrichment with calcium and magnesium ions and depletion of

sodium ions can be due to the process of dolomitization and halite deposition (Ghabayen et al., 2006).
The values of the described ion ratios are presented in Table 2. Based on the results of these ionic ratios, the groundwater salinity in the study area is affected by the gypsum and salt sediments of the Lower and Upper Red Formation and evaporation during the dry period.

Moreover, $\frac{Ca^{2+}}{HCO_3^- + SO_4^{2-}}$ ion ratio is less than 1 and $\frac{Mg^{2+}}{Ca^{2+}}$ ion ratio has low values, so, it is more likely to be affected by saline waters in deeper aquifer areas. It should be noted that a closer look at this issue requires more information.

Gibbs diagram of groundwater

Drawing TDS values vs. ionic ratios and groundwater can provide useful information on natural processes affecting water composition (Gibbs, 1970). According to Gibbs diagram, the chemical quality of the studied waters is affected by two factors of evaporation - sedimentation and aquifer reservoir nature (Figures 10 and 11). Because of the increase in the TDS content of water, the concentration of sodium and chloride ions are more effective than the concentration of bicarbonate and calcium ions. In addition, the positive correlation between sodium and chlorine ions and water TDS indicates that water salinity increases under the influence of evaporation-deposition process (Figures 11 and 12). In arid and semiarid environmental conditions, human activities also influence the role of the evaporation process by increasing the amounts of sodium and chlorine ions and thereby increasing the TDS content of water.

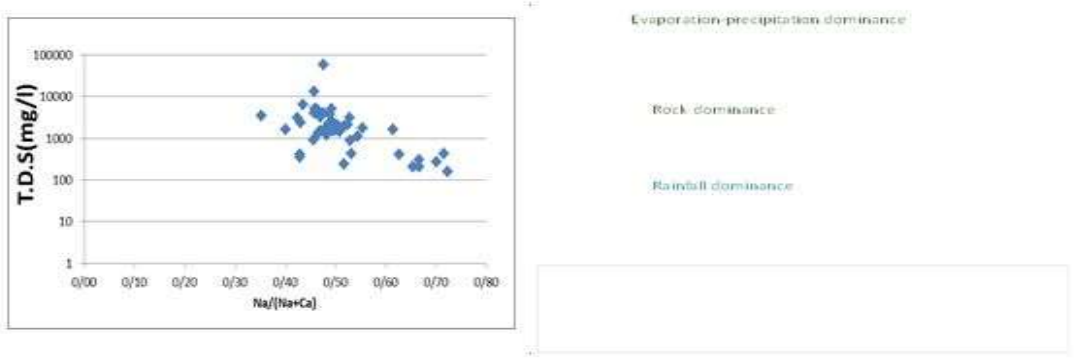

Figure 10. Gibbs diagram showing the geochemical processes governing the region.

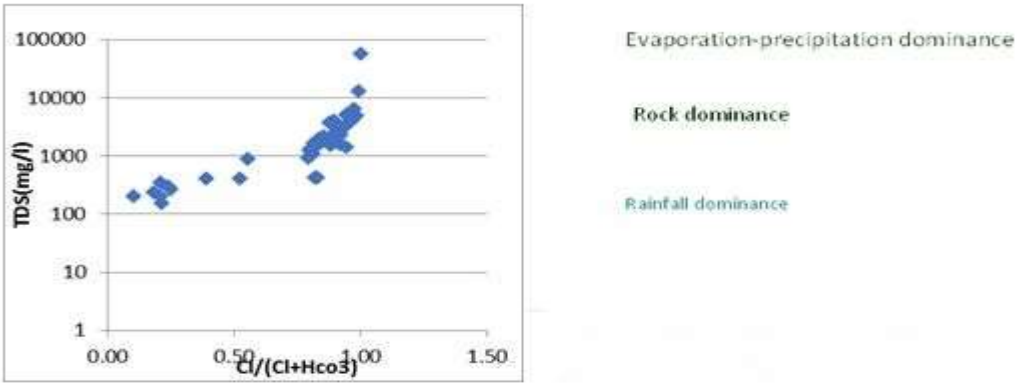

Figure 11. Gibbs diagram showing the geochemical processes governing the study area

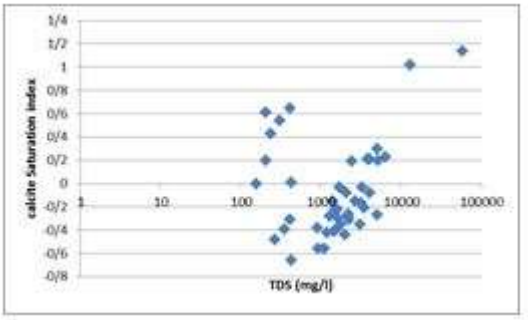

Figure 12. Calcite saturation index of groundwater in the study area in March 2018

Saturation indexes

In order to evaluate the hydrogeochemistry of water in the study area, the values of the saturation indexes of the samples were calculated towards calcite, dolomite, and gypsum for the samples taken in October and March of 2017-2018 using the PHREEQC computer program (Parkhurst and Appelo, 2005). The results of the March calculations are presented in Table 3.

Table 3. Saturation indexes of the study area in March 2018

Sample	SI (Anhydrite)	SI (Aragonite)	SI (Calcite)	SI (CO2)(g)	SI (Dolomite)	SI (Gypsum)	SI (H2)(g)	SI (H2O)	SI (halit)	SI (O2)(g)	SI (Sylvite)
W1	-0.98	-0.41	-0.27	-2	-0.76	-0.64	-22.04	-1.61	-4.18	-40.56	-5.69
W2	-1	-0.22	-0.08	-1.84	-0.11	-0.65	-24.	-1.6	-4.3	-40.	-5.9

							04	1	8	56	
W3	-0.63	0.09	0.23	-1.8	0.38	-0.3	22.04	-1.58	-4.05	-40.22	-5.49
W4	-0.61	0.016	0.3	-1.6	0.61	-0.26	-22.04	-1.63	-4.2	-40.91	-5.68
W5	-1.17	0.04	0.19	-1.59	0.39	-0.8	-22.04	-1.66	-4.7	-41.26	-6.12
W6	-1.11	-0.18	-0.03	-1.67	-0.07	-0.75	-22.04	-1.63	-4.75	-40.91	-6.29
W7	-0.85	-0.13	0.2	-1.69	0.05	-0.5	-22.04	-1.63	-4.46	-40.91	-5.89
W8	-1.36	-0.23	-0.08	-1.61	-0.28	-0.98	-22.04	-1.69	-5.05	-41.62	-6.49
W9	-1.31	-0.42	-0.28	-1.87	-0.58	-0.98	-22.04	-1.58	-4.51	-40.22	-6.17
W10	-1.81	-0.36	-0.22	-1.64	-0.53	-1.46	-22.04	-1.61	-5.13	-40.56	-6.59
W11	-1.5	-0.5	-0.35	-1.71	-0.75	-1.15	-22.04	-1.63	-4.5	-40.91	-6.19
W12	-1.44	-0.46	-0.31	-1.78	-0.73	-1.09	-22.04	-1.61	-4.81	-40.56	-6.42
W13	-1.41	0.07	0.21	-1.4	0.69	-1.07	-22.04	-1.61	-4.43	-40.56	-5.74
W14	-1.33	-0.3	-0.15	-1.63	-0.21	-0.97	-22.04	-1.63	-4.81	-40.91	-6.33
W15	-1.26	-0.35	-0.21	-1.74	-0.66	-0.92	-22.04	-1.58	-4.37	-40.22	-6.1
W16	-1.5	-0.56	-0.41	-1.84	-0.99	-1.12	-22.04	-1.69	-5.29	-41.62	-6.77
W17	-1.33	-0.41	-0.26	-1.74	-0.44	-0.99	-22.04	-1.61	-4.94	-40.56	-6.47
W18	-1.38	-0.43	-0.29	-1.88	-0.75	-1.01	-22.04	-1.66	-5.28	-41.26	-6.75

W19	-1.3	-0.57	-0.42	-1.94	-1.3	-0.92	-22.04	-1.69	-5.66	-41.62	-7.09
W20	-1.33	-0.37	-0.22	-1.77	-0.64	0.94	22.04	-1.71	-5.44	-40.56	-6.77
W21	-1.6	-0.71	-0.56	-1.88	-1.1	-1.26	-22.04	-1.58	-5.83	-40.21	-7.08
W22	-1.39	-0.55	-0.4	-1.88	-0.89	-1.03	22.04	-1.63	-5.34	-40.91	-6.9
W23	-1.34	-0.29	-0.15	-1.7	-0.43	-0.98	-22.04	-1.66	-5.46	-41.11	-6.73
W24	-1.42	-0.42	-0.28	-1.76	-0.66	-1.08	-22.04	-1.61	-5.5	-40.56	6.81
W25	-1.21	-0.18	-0.03	-1.76	-0.16	-1.08	-22.04	-1.61	-5.5	-40.56	6.81
W26	-1.5	-0.7	-0.56	-1.86	-1.21	-1.12	-22.04	-1.69	-5.39	-41.62	-6.82
W27	-0.72	0.06	0.21	-1.52	0.51	-0.36	-22.04	1.63	-4.62	-40.91	-6.33
W28	-0.95	-0.32	-0.17	-1.86	-0.35	-0.62	22.04	-1.58	-4.98	-40.22	-6.44
W29	-1.45	-0.5	-0.35	-1.79	-0.74	-1.09	-22.04	-1.63	-5.42	-40.91	-6.77
W30	-1.36	-0.59	-0.44	-1.83	-0.73	-1.02	-22.04	-1.61	-5.11	-40.56	-6.57
W31	-1.14	-0.14	0.01	-1.58	0	-0.78	-22.04	-1.63	-5.13	-40.91	-6.5
W32	-0.37	0.99	1.14	-3.32	2.27	-0.01	-24.03	-1.76	-1.61	-38.38	-3.01
W33	-0.61	0.96	1.02	-2.82	2.02	-0.26	-24.04	-1.64	-3.26	-36.92	-4.95
W34	-2	-0.81	-0.66	-1.79	-1.38	-1.6	-22.03	-1.74	-6.39	-42.33	-7.37
W35	-2.25	-0.45	-	-	-0.62	-1.9	-	-	-	-	-

			0.31	1.61			22.04	1.63	7.82	40.91	8.14
W36	-2.8	-0.15	0	-2.97	-0.25	-2.41	24.04	-1.71	-8.33	-37.97	-8.81
W37	-1.54	0.28	0.43	-2.99	0.72	-1.13	-24.03	-1.74	8.09	-38.33	-8.65
W38	-2.43	0.01	0.61	-2.96	-0.18	-2.03	-24.03	-1.74	-8.14	-38.33	-8.14
W39	-2.46	0.05	0.2	-2.92	-0.22	-2.06	-24.03	-1.74	-7.95	-38.33	0
W40	-2.11	0.5	0.65	-2.67	0.99	-1.72	-24.04	-1.71	-7.43	-37.97	-8.27
W41	-2.35	-0.63	-0.48	-1.76	-1.44	-1.96	-24.03	-1.71	-7.72	-41.97	0
W42	-2.9	0.39	0.54	-2.69	0.83	-2.5	-24.03	-1.74	-8.2	-38.33	-8.93
W43	-2.36	-0.54	-0.39	-1.63	-0.79	-1.97	-22.04	-1.71	-7.97	-41.97	-8.56
W44	-1.77	-0.53	-0.38	-1.7	-0.85	-1.38	-22.04	-1.71	-6.5	-41.97	-7.32

The saturation index (SI) of the groundwater qualitatively describes the deviation of the chemical composition of the groundwater from equilibrium with respect to the dissolved minerals (Appelo and Postma, 2005; Drever, 1997). Since the saturation state is indicative of hydrogeochemical processes, when the saturation indexes of a mineral are positive and negative, the deposition and dissolution processes can be expected, respectively (Appelo and Postma, 2005) Water samples' saturation studies in October and March of 2017-2018 show that almost all groundwater samples and the ranges are over saturated with calcite and dolomite, saturated in HableRood inlets, and under saturation with gypsum and halite, respectively. This shows the importance of the effect of carbonate minerals on the underground water chemistry of this area (Figures 13-15). Approximately 69% of the samples under study were over-saturated with calcite and dolomite, therefore, the expected process is calcite and dolomite deposition. However, the negative Gypsum and Halite saturation index is indicative of continued dissolution of the mineral by water. As the concentration of sulfate ion in the water increases, the amount of saturated gypsum index in the groundwater increases. Dissolution of the gypsum affected by H_2CO_3 or alkaline water causes the calcite to deposit, because gypsum is more soluble than calcite.

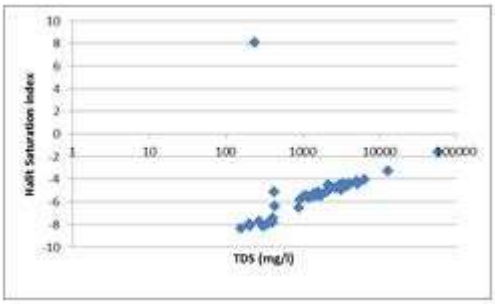

Figure 13. Halite saturation index of groundwater in the study area in March 2018

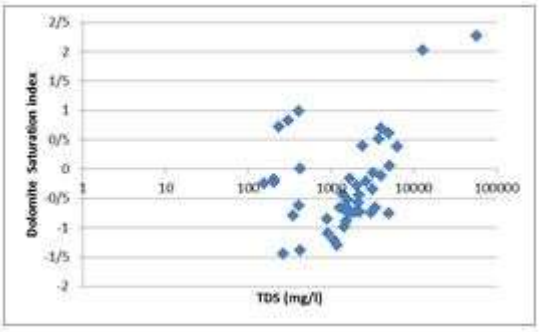

Figure 14. Dolomite saturation index of groundwater in the study area in March 2018

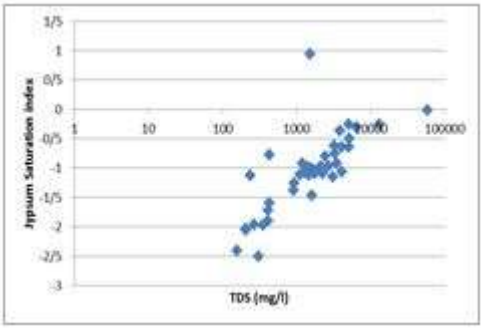

Figure 15. Gypsum saturation index of groundwater in the study area in March 2018

Conclusion and Suggestions

The results of hydrogeochemical and groundwater contamination studies are as follows:

1) Based on the Piper, Durov, and Stiff diagrams, the waters of the study area are of three types of bicarbonate, sulfate, and chlorinated and the facies of all studied samples are calcic and sodic. In addition, the type of most waters in the northern part is bicarbonate while it is sulfated in the middle part and chlorinated in the aquifer outlet.
2) The results of the combined diagrams show that the dissolution of gypsum, halite, and cation exchange process are the dominant geochemical processes in the groundwater composition. The origin of evaporites in this area can be gypsum, salt, and marl sediments of the Upper Red Formation (Figures 16-18).

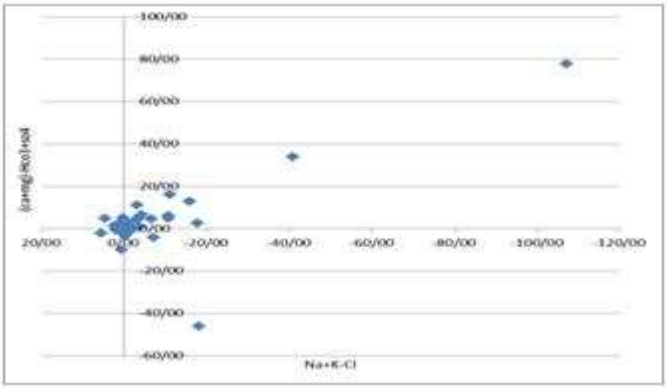

Figure 16. Combined diagram showing the process of ionic exchange of water

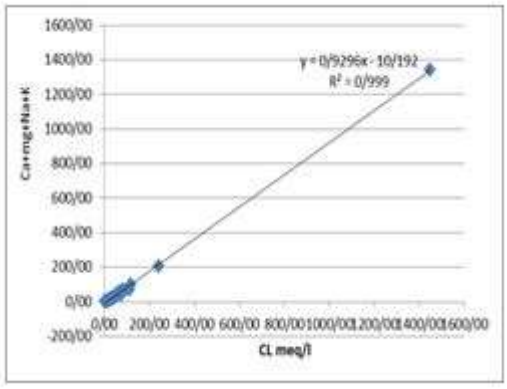

Figure 17. Combined diagram showing the effect of dissolution of chloride salts on the waters of the study area

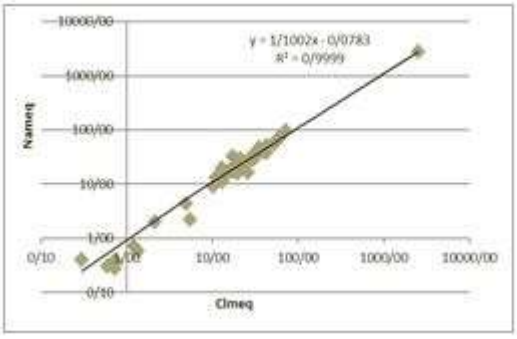

Figure 18. Combined diagram of sodium vs. chlorine.

3) Examination of the ionic ratios indicates that the aquifer reservoir stone nature is of limestone and dolomite. In addition, groundwater salinity in the area may be affected by the Lower and Upper Red Formation.
4) The results of the correlation analysis show that the low correlation coefficient of HCO_3^- and TDS and EC of the groundwater in the study area shows that this anion is insignificant in increasing the mentioned parameters. Also, the high correlation coefficient among Cl^- , Na^+ , and SO_4^{2-} constituents can indicate that they are of the same origin (Figures 19 and 20).

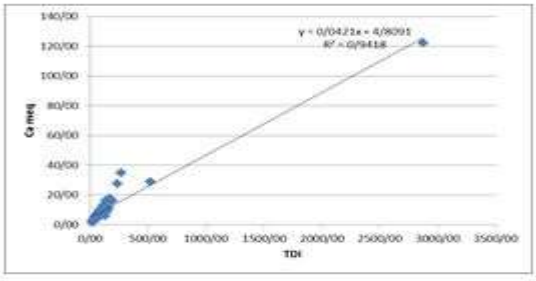

Figure 19. Combined diagram of calcium vs. total soluble ions in the region.

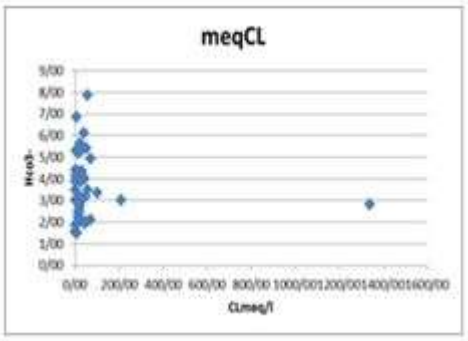

Figure 20. Combined diagram of bicarbonate vs. chlorine.

5) Based on the results of the measurements it can be concluded that the average annual concentration of chloride and sodium in the groundwater of this area is affected by a single geological source (halite). Because the dissolution of this mineral enters a similar proportion (one mole) of chlorine and sodium to the water while the similarity between the amounts of sulfate, chloride, and sodium in the study area indicates the dissolution of evaporite rocks (gypsum and salt).
6) The analysis of the main components of groundwater chemical variables in the study area shows that most of the total variance of groundwater composition in this area is controlled by three main components. The first principal component is attributed to a set of geochemical processes (dissolution and ion exchange). The second major component is the chemical variables that are on the bicarbonate anion. It can therefore be attributed to an atmospheric origin. The third factor that has the least impact on the composition of the free aquifer is attributed to surface activities (such as agricultural activities) that are widely practiced in the region. This factor has been identified considering the high nitrate level and lack of lithological origin of nitrate and effect of leaching of agricultural fertilizers on concentration, infiltration of urban wastewater, and absorbance wells' wastes.
7) In Garmsar and northwest of the alluvial fan, the electrical conductivity is generally over 2000 μmbos/cm; it even reaches 11200 μmbos/cm in the northwest of Ghias Abad village. The reason for the increase in EC can be attributed to the presence of a geological factor. Since the samples collected from these points are from wells with more than 80 meters depth, it can be concluded that due to contact with the Red Formation salts, the water begins to dissolve between the gypsum and evaporite layers, thus causing deep water salinity in the area.
8) The $[HCO_3]/[Cl]$ ratio is useful for determining the direction of groundwater flow and the distance of a sample of water from the feeding site. This ratio decreases in the direction of flow due to more dissolution of chlorine. In the northern part of Firozkooh watershed, Gursefid River, this ratio is 13, and in the ending part of HablehRood River, i.e. Gholamabad, the water content is zero (Figure 21).

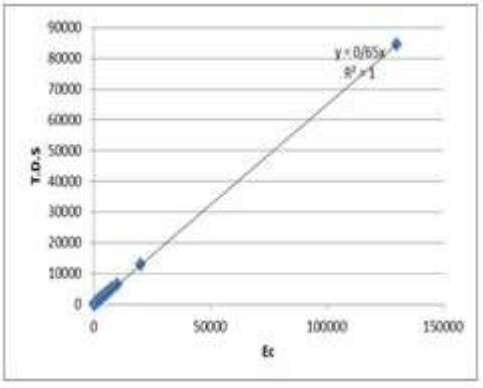

Figure 21. Relationship between electrical conductivity and total soluble solids.

9) The highest amounts of bicarbonate in the studied waters were measured in HablehRood watershed. The study of temporal variations of bicarbonate

concentration of groundwater in the area shows that unlike chloride, bicarbonate ion has the lowest coefficient of variation during sampling periods.
10) The measurement of nitrate ion concentration in the aquifer during the two sampling periods indicates that its concentration is often less than 25 mg/l. This may be due to the slow vertical mixing in the saturation zone, which causes different concentrations of nitrate to enter the aquifer along the same flow path. In addition, very low nitrate concentrations (5 mg/l) in some places are due to the dense soil and the variability of feeding conditions, because soil density decreases the thickness of the ventilation zone and results in anaerobic conditions in the deeper parts of the soil (Figures 22 and 23).

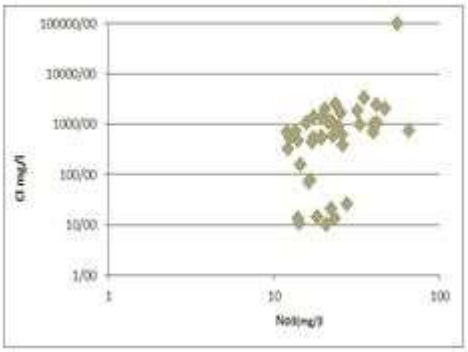

Figure 22. Logarithmic diagram of chlorine vs. nitrate in March 2018.

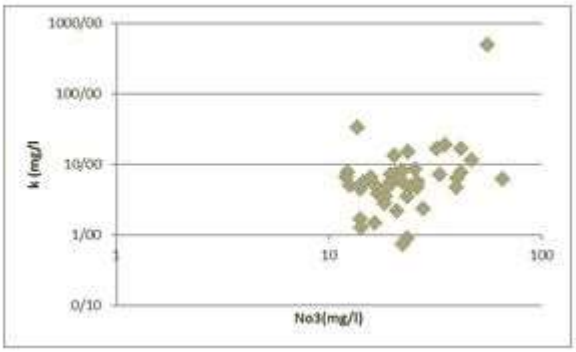

Figure 23. Logarithmic diagram of potassium vs. nitrate in March 2018.

Suggestions

a. The high nitrate level (20 mg/l) in the study area can be indicative of the beginning of the aquatic contamination. Therefore, serious measures to prevent water pollution should be considered now. With regard to nitrate, 65 mg/l in Garmsar municipality well, sewage project should be implemented.
b. Controlling the use of fertilizers and pesticides and implementing modern methods of plant pest controlling measures.

c. Finding the appropriate location for establishing municipal and industrial waste disposal centers, and applying appropriate design for waste disposal sites.
d. Finding the proper location of industrial, agricultural, and population centers according to the principles of land preparation.
e. Creating and protecting the privacy of water wells, with an emphasis on urban and rural drinking water wells and preventing the spread of industries around these areas.

Acknowledgments

I would like to thank Mr. Dr. Gholamhossein Karami Associate Professor of Shahroud University of Technology, and Mr. Alireza Abuotrabi, the official for groundwater management at Semnan Provincial Water Company for his academic support.

Funding

This research did not receive any specific grant from funding agencies in the public, commercial, or Not for-profit sectors.

Conflict of interest: The authors declare that they have no conflict of interest.

References

Aghanabati, A., 2011. Geology of Iran. Geological Survey and Mineral Exploration of Iran.

Anderson, T.W., Welder, G.E., Lesser, G., Trujilo, A., 1988. Region 7, Central alluvial basin. In: Back, W., Rosenbein, J.S., Seaber, P.R. (Eds.), Geology of North America (hydrology). pp. 81-86.

Appelo, C.A.J., Postma, D., 2005. Geochemistry, Groundwater and Pollution, Brookfield, Vermont Balkema.

Berberian, M., King, G., 1981. Towards a Paleogeography and Tectonic Evolution of Iran, Canadian Journal of Earth Sciences, 18, 210-265. https://doi.org/10.1139/e81-019

Berner, E.K., Berner, R.A., 1987. The Global Water Cycle. Prentice Hall, Englewood Cliffs.

Busby, J.F., Plummer, L.N., Lee, R.W., Hanshaw, B.B., 1991. Geochemical Modeling of the Madison Aquifer in Parts of Montana, Wyoming, and South Dakota. Water Resources Research, 26(9), 1981-2014. https://doi.org/10.1029/WR026i009p01981

Cetinag, B., Okan, O.O. 2003. Hydrochemical characteristics and pollution potential of Uluova aquifers, Elazig, Turkey. Environmental Geology. 45, 796-807. https://doi.org/10.1007/s00254-008-1357-2

Drever, J.I., 1997. The Geochemistry of Natural Waters. Prentice Hall.

Faryabi, M., Kalantari, N., Negarestani, A., 2010. Evaluation of factors influencing groundwater chemical quality using statistical and hydrochemical methods in Jiroft plain. Scientific Quarterly Journal of Geosciences, 20(77), 115-120. https://doi.org/10.22071/gsj.2010.55355

Fatima, A., Khaliq, S. A., & Khan, R. (2021). Bacteriological Analysis of Drinking Water from Different Regions of Karachi from February 2016 to August 2016. Archives of Pharmacy Practice, 12(4), 25-8.

Flak, A., Anna Mencio, A., Caminal, R.P., Soler Gil, A., Mas-Pla, J., 2011. Groundwater development effects on different scale hydrogeological systems using head, hydrochemical and isotopic data and implications for water resources management: The Selva basin (NE Spain), pp. 378.

Ghabayen, S.M.S., McKee, M., Kemblowski, M., 2006. Ionic and isotopic ratios for identification of salinity sources and missing data in the Gaza aquifer, Journal of Hydrology, 318, 360-373.

Hassanin, SO., Taher, A., Mustafa, ME., & Nadir, AS. (2019). A Comparative Study between Effect of Physical Activity and ADAM, Vs Iron Salts on Some Physical Traces of Underground Water. International Journal Pharmaceutical Research & Allied Sciences, 8(3), 37-46.

Hounslow, A.W., 1995. Water Quality Data: Analysis and interpretation, Lewis Publisher.

Jalali, M., 2005. Major ion chemistry in the Bahar area, Hamedan, western Iran, Environmental Geology, 47, 763-772.

Jalali, M., 2007. Hydrochemical Identification of Groundwater Resources and Their Changes under the Impacts of Human Activity in the Chah Basin in Western Iran. Environmental Monitoring and Assessment, 130(1-3), 347-364.

Mazor, E., Nativ, R., 1992. Hydraulic Calculation of Groundwater Flow Velocity and Age: Examination of the Basic Premises. Journal of Hydrology, 138, 211-222. http://dx.doi.org/10.1016/0022-1694(92)90165-R

Montoroi, J.P., Grünberger, O., Nasri, S., 2002. Groundwater geochemistry of a small reservoir catchment in Central Tunisia. Applied Geochemistry, 17(8), 1047-1060.

Parkhurst, D.L., Appelo, T., 1999. User's guide to PHREEQC version 3 - a computer program for speciation, batch-reaction, one-dimensional transport, and inverse geochemical calculations. U.S. Geological Surve.

Piper, A.M., 1953. A graphic procedure in the geochemical interpretation of water analysis. USGS Groundwater Note.

Richter, B.C., Kreitler, W.C., 1993. Geochemical Techniques for Identifying source of Groundwater Salinitization. CRC Press, New York.

Rosen, M.R., Lapham, W.W., 2008. Introduction to the US Geological Survey National Water-Quality Assessment (NAWQA) of ground-water quality trends and comparison to other national programs. Journal of Environmental Quality, 37, 190.

Sami, K., 1992. Recharge mechanisms and geochemical processes in a semi-arid sedimentary basin, Eastern Cape, South Africa. Journal of Hydrology, 139(1-4), 27-48.

Sancho, A.F., 2010. Geological and human influences on groundwater flow systems in range-and-basin areas: the case of the Selva Basin (Catalonia, NE Spain). PhD dissertation, Universitat Autònoma de Barcelona.

Sandow Mark, Y., 2009. RETRACTED ARTICLE: The hydrochemical framework of surface water basins in southern Ghana. Environmental Geology, 57(4), 789-796.

Sasamoto, H., Yui, M., Arthur, R.C., 2004. Hydrochemical characteristics and groundwater evolution modeling in sedimentary rocks of the Tono mine, Japan. Physics and Chemistry of the Earth, Parts A/B/C, 29(1), 43-54.

Schwartz, F.W., Zhang, H., 2003. Fundamentals of Groundwater, John Wiley and Sons.

Sikdar, B., Kalyanaraman, S., Vastola, K.S., 2001. An integrated model for the latency and steady-statethroughtput of top connections, Performance Evalauation, 46(2-3), 139-154.

Spears, D.A., 1986. Mineralogical control of the chemical evolution of groundwater. Solute processes, Chichester: Wiley.

Stocklin, J., 1968. Structural history and tectonics of Iran: A review, AAPG Bulletin, 52, 1229-1258.

Van der Weijden, C.H., Pacheco, F.A., 2003. Hydrochemistry, weathering and weathering rates on Madeira island. Journal of Hydrology, 283(1-4), 122-145.

Vengosh, A., Spivack, A.J., Artzi, Y., Ayalon, A., 1999. Geochemical and boron, strontium, and oxygen isotopic constraints on the origin of the salinity in groundwater from the Mediterranean coast of Israel. Water Resources Research, 35, 1877-1894.

Wen, X., Wu, Y., Su, J., Zhang, Y., Liu, F., 2005. Hydochemical characteristic and salinity of groundwater in the Ejina Basin, Northwestern China. Environmental Geology, 48, 665-675.

Yates, M.V., 1985. Septic tank density and groundwater contamination, Groundwater, 23, 586-591.